

# THE 4TH INTERNATIONAL CONFERENCE ON ALUMINUM ALLOYS

## ALPHA-PHASE PARTICLES IN 6XXX ALUMINUM ALLOYS

P. Donnadieu<sup>1</sup>, G. Lapasset<sup>2</sup>, B. Thanaboonsombut<sup>3</sup>, T.H. Sanders Jr.<sup>3</sup>

<sup>1</sup> Laboratoire d'Etude des Microstructures, CNRS/ONERA, BP 72, 92322 Châtillon France

<sup>2</sup> ONERA, BP 72, 92322 Châtillon - France

<sup>3</sup> School of Materials Science and Engineering, Georgia Institute of Technology - Atlanta, GA 30332-0245 - USA

### Abstract

We report a transmission electron microscopy study of the microstructure of 6XXX aluminum alloys. Our investigations focus on the Mn and Fe containing phases. Two types of phases are identified. Though they both belong to the alpha-type  $Al_{12}(Fe, Mn)_3Si$  phase, they mostly differ by their Mn/Fe ratio. The coarse alpha-phase particles are Fe-rich while the dispersoids alpha-phase particles are Mn-rich. Selected area diffraction patterns taken on the coarse particles show a noticeable diffuse scattering due to short range ordering. This ordering effect is reinforced by the Mn additions. Regarding the alpha-phase dispersoids, we have determined that they show several types of orientation relationships with the matrix.

### Introduction

Manganese additions to 6XXX aluminum alloys are made to improve the resistance to recrystallization of rolled and heat treated products [1]. Although iron is not an intentional addition to aluminum, it is virtually present in all aluminum alloys as an impurity. Because of the strong interaction between manganese and iron, the role of iron must be considered when studying the influence of the manganese additions [1]. In the 6013 alloy, there are two types of phases that contain, besides Al and Si, manganese and iron. Though they both belong to the  $Al_{12}(Fe, Mn)_3Si$  family, they differ in several respects. First, their Mn and Fe contents are very different. Second, the Mn-rich phases (often called dispersoids) are small particles formed inside the matrix by solid state precipitation during ingot preheating. On the contrary, the Fe-rich phases are coarse particles formed during solidification in the interdendritic channels. The present work reports a TEM investigation of these two kinds of phases in series of 6013 alloys to which various additions of Mn and Fe have been made. Special attention will be paid to the partition between manganese and iron and to the crystallography of these particles.

### Experimental conditions

The five alloys studied here are compositional variants of 6013 since the amounts of Cu, Si and Mg were fixed at nominal levels of 6013 (Table 1).

Table 1: Composition of 6013 variants in weight per cent.

Identification	Si	Fe	Cu	Mn	Mg	Al
62-0.2 Mn	0.71	0.28	1.01	0.21	0.87	bal.
62-0.8 Mn	0.69	0.23	0.99	0.80	0.89	bal.
74-0.55 Mn	0.73	0.25	0.96	0.55	0.88	bal.
77-0.2 Fe	0.70	0.20	1.01	0.66	0.90	bal.
76-0.1 Fe	0.73	0.09	1.04	0.42	0.94	bal.

The processing of these alloys was described elsewhere [1]. All these alloys have been preheated, hot rolled and solution heat treated before the TEM investigations. Slices cut from these alloys were mechanically polished down to a thickness less than 100 microns. Subsequently, the foils were electropolished in a double-jet electropolishing device (T=35°C, electrolyte: 1/3 nitric acid, 2/3 methanol).

Chemical analysis (EDS) was performed on a JEOL 4000 FX electron microscope equipped with a KEVEX Energy Dispersive X-ray spectrometer. The atomic ratio Mn/Fe (where Mn and Fe contents are in at%) was estimated through a standardless quantification of spectra. This ratio was assumed to be nearly insensitive to absorption. As far as only dispersoids are concerned, the spectra contain a contribution from the surrounding matrix. But this contribution was not considered to alter significantly the ratio Mn/Fe since solubilities of Mn and Fe within the Al matrix are rather low. The crystallographical study and the EDS analysis have been performed on the same TEM samples.

### The coarse AlMnFeSi particles

TEM images (Figure 1) show that the coarse particles often form aggregates which are elongated in the rolling direction. Their composition can be described by  $Al_{12}(Fe, Mn)_3Si$ . The Mn/Fe ratio in these particles strongly depends on the nominal composition of the starting alloy, as shown previously [1]. In the various alloys studied here, the Mn/Fe atomic ratio of the coarse particles ranges from 0.2 to 1.

The crystallographic information given by the electron diffraction patterns (EDPs) shows that the structure is cubic with a lattice parameter  $a=1.27$  nm and a  $Im\bar{3}$  space group. Chemical composition and crystallographic data suggest that this phase is reminiscent of the  $\alpha$ -AlFeSi phase [2]. The  $\alpha$ -AlFeSi phase is nearly isostructural to the  $\alpha$ -AlMnSi phase [3] except that the AlFeSi phase belongs to the  $Im\bar{3}$  space group while the AlMnSi phase is a

Figure 1: Typical aspect of the alpha-phase particles formed in the interdendritic channels.

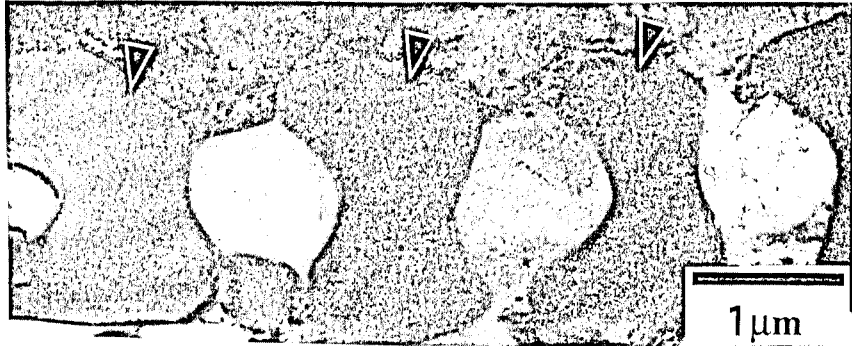


Figure 2: Sequence of EDPs taken of interdendritic alpha-phase. Note the rings of diffuse intensity in the  $\langle 001 \rangle$  and  $\langle 011 \rangle$  zone axis patterns. The  $\langle 111 \rangle$  zone axis EDP only exhibits a few amount of diffuse scattering as indicated by the arrow outside the zero order Laue zone.

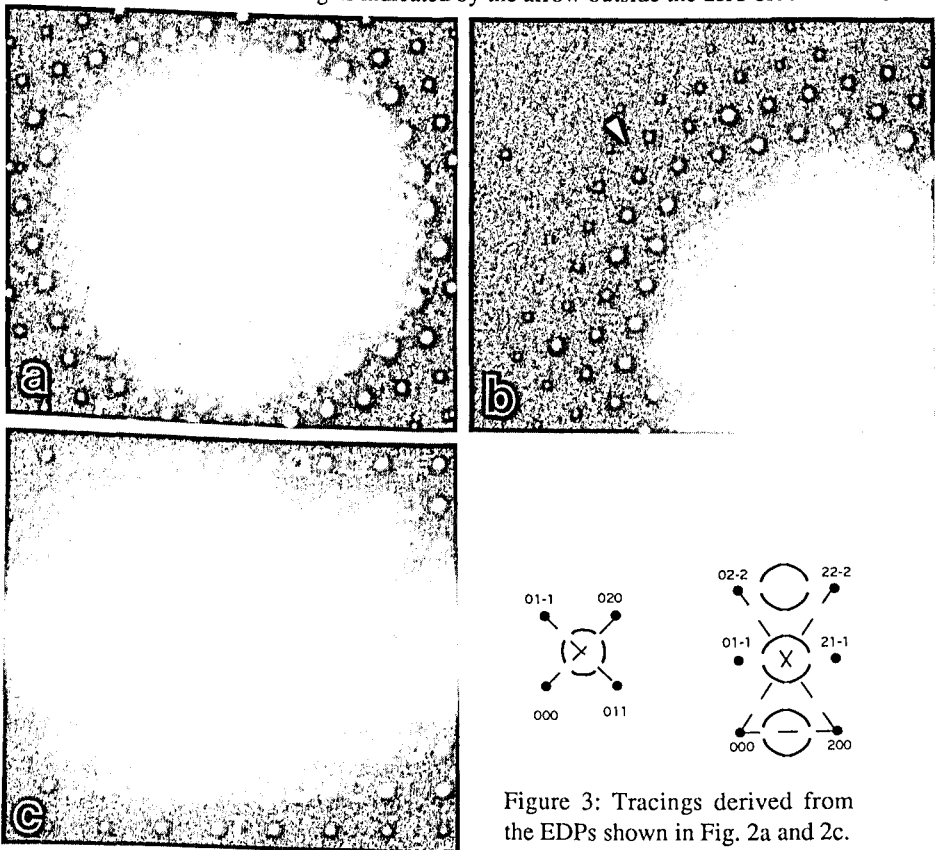


Figure 3: Tracings derived from the EDPs shown in Fig. 2a and 2c.

Pm3 structure. As shown by Cooper and Robinson and confirmed by more recent studies [4] the alpha-phase cubic cell contains 138 atoms that essentially separate in Mackay icosahedra and glue atoms connecting them. The Mackay icosahedra are aggregates of 54 atoms packed in several successive icosahedral and dodecahedral shells [5]. In the alpha-phase, the Mackay icosahedra are centered at the nodes of a body centered cubic structure. Actually Cooper and Robinson have shown that there are two types of aggregates. The aggregate at the 000 node and the one at the  $1/2 \ 1/2 \ 1/2$  node are not identical because one of them has a vacant Aluminum site. These two different Mackay icosahedra being packed on an ordered BCC lattice, the alpha AlMnSi phase has a Pm3 space. In the alpha AlFeSi phase, the two types of icosahedra have been also identified but they are not packed in an ordered way on the BCC lattice. Therefore the symmetry group is larger (Im3 instead of Pm3). The alpha-AlFeSi phase is then described as a disordered cubic packing of the two types of Mackay icosahedra while the alpha AlMnSi phase is an ordered packing.

Besides the structure identification, electron diffraction reveals a very attractive property in direct connection with the manganese and iron content. Figure 2 displays several diffraction patterns taken in a particle exhibiting a Mn/Fe ratio roughly equal to 1 (this particle was found in the 76-0.1 Fe variant). On each zone axis pattern, respectively a  $\langle 001 \rangle$  zone axis (Figure 2a) and a  $\langle 011 \rangle$  zone axis (Figure 2c), one can note rings of diffuse scattering. The rings are actually formed of several arcs of intensity. In both cases it is remarkable that, as indicated in the tracing shown in Figure 3, there is no diffuse scattering in the  $\langle 001 \rangle$  directions. The  $\langle 111 \rangle$  zone axis EDP shows only a little amount of diffuse scattering forming small triangles, and not rings, outside the zero order Laue zone (Figure 2b). Diffraction patterns taken along other zone axes allow to conclude that in the reciprocal space, the diffuse scattering forms a surface which is close to a cube-octahedron. We have analyzed this effect with more details elsewhere [6].

Such diffuse scattering is related to the establishment of short range order. In the present case, the alpha phase structure suggests that the entities concerned by the ordering are the two types of Mackay icosahedra. Actually, whatever would be the entities involved in the ordering phenomenon, the point is that the Manganese content has an influence on ordering as illustrated by the EDPs in Figure 4. The EDS chemical analysis yields, respectively, a Mn/Fe ratio close to 0.2 for the alpha-phase exhibiting the EDP shown in Figure 4a (this particle was found in the 62-0.2 Mn variant) and a ratio close to 1 for the particle giving the EDP shown in Figure 4b. The diameter of the diffuse intensity ring becomes larger when the Mn/Fe ratio significantly decreases.

It stems that Manganese favors the establishment of a long range ordering. Therefore manganese is likely mediating a continuous transition between the Im3 and the Pm3 alpha-AlMnSi phase. In other words, one may find alpha-AlFeMnSi phase with any proportion of manganese and iron.

Regarding microstructural features, it suggests that the coarse alpha-phase particles are able to contain a significant quantity of the added manganese. Regarding recrystallization, the coarse

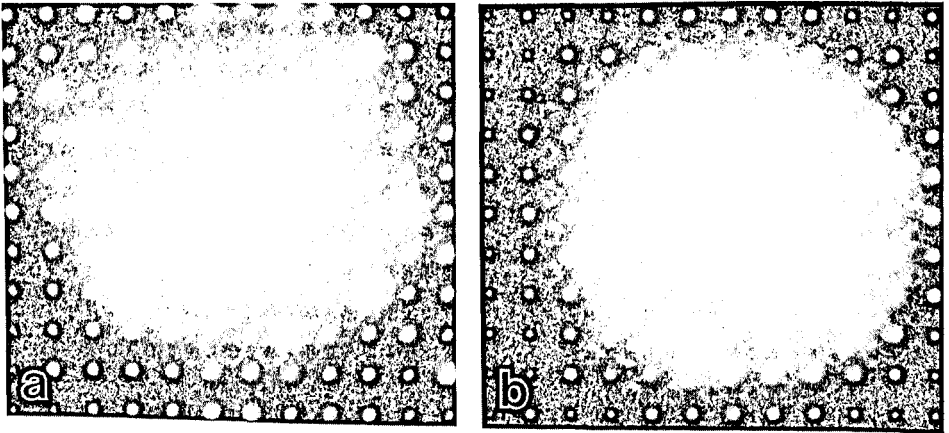


Figure 4:  $\langle 001 \rangle$  zone axis EDPs taken in alpha-phase particles of different Mn and Fe contents; Mn/Fe = 0.2 (Fig.4a), Mn/Fe = 1 (Fig.4b)



Figure 5: Typical morphology of the alpha-phase dispersoids. Note that the dispersoids which are mostly round shaped might be also sometimes slightly faceted.

alpha-phase particles provide preferential sites for nucleation. Therefore lowering the Fe content and avoiding a too high level of Manganese will be beneficial for the resistance to recrystallization.

### The alpha-phase dispersoids

The dispersoids had formed during the preheat [1]. These particles are quite small (0.1 to 0.3  $\mu\text{m}$ ) and usually without any remarkable shape (Figure 5). Their composition is generally thought to be well described by the formula:  $\text{Al}_{12}\text{Mn}_3\text{Si}$ . Nevertheless they do contain some Fe. EDS analysis reveals that, in a same alloy, the dispersoid Mn/Fe ratio is quite variable regardless of the nominal composition of the alloy. However, because of the small size of the particles, it is not possible to give an accurate Mn/Fe ratio. In all the alloys studied here, this ratio is larger than 3. Sequences of electron diffraction patterns show that the Mn-dispersoids have a Pm3 cubic structure with a cell parameter close to 1.27 nm. Crystallographical data are then in agreement with an alpha-AlMnSi phase.

From the microstructural point of view, these particles have a remarkable property. They do not show simple orientation relationships (OR) with the aluminum matrix as illustrated by the sequence of EDPs shown in Figure 6. These four patterns have been recorded on several particles. Each of them allows to fully determine one OR. These four OR, which are not variants of each other, can be described as follows:

OR n°1:  $[001]_{\alpha} // [111] \text{ Al}$   
 $[100]_{\alpha} // [2-1-1] \text{ Al}$   
 $[010]_{\alpha} // [01-1] \text{ Al}$

OR n°2:  $[001]_{\alpha}$  close to  $[-130] \text{ Al}$   
 $[100]_{\alpha} // [31-1] \text{ Al}$   
 $[010]_{\alpha}$  close to  $[103] \text{ Al}$   
 or  $[0-11]_{\alpha} // [011] \text{ Al}$

OR n°3:  $[001]_{\alpha}$  close to  $[130] \text{ Al}$   
 $[100]_{\alpha}$  close to  $[3-12] \text{ Al}$   
 $[010]_{\alpha}$  close to  $[2-1-3] \text{ Al}$   
 or  $[111] // [31-1]$

OR n°4:  $[001]_{\alpha}$  close to  $[-231] \text{ Al}$   
 $[100]_{\alpha} // [11-1] \text{ Al}$   
 $[0-10]_{\alpha}$  close to  $[213] \text{ Al}$   
 or  $[-111] // [-100]$

These OR have a common point: they put very few symmetry elements in common between the matrix and the dispersoids. Therefore a large number of variants will be generated (24 variants for each OR). In all recorded cases, the dispersoid and the matrix have a two-fold axis in common, therefore the particles are expected to be somewhat faceted. Besides, the diffraction patterns show that no particular coherence is related to these ORs. Consequently the dispersoids are not expected to be large. Actually we do observe that the dispersoids are slightly faceted and keep a quite small and regular shape (Figure 5).

In other words the numerous orientation variants and the absence of coherence provide the basis for an interesting metallurgical behavior. On the one hand, numerous orientation variants give to the dispersoids a peculiar efficiency in the pinning of grain boundaries. On the other hand, the absence of coherence avoids the formation of needle shaped precipitates

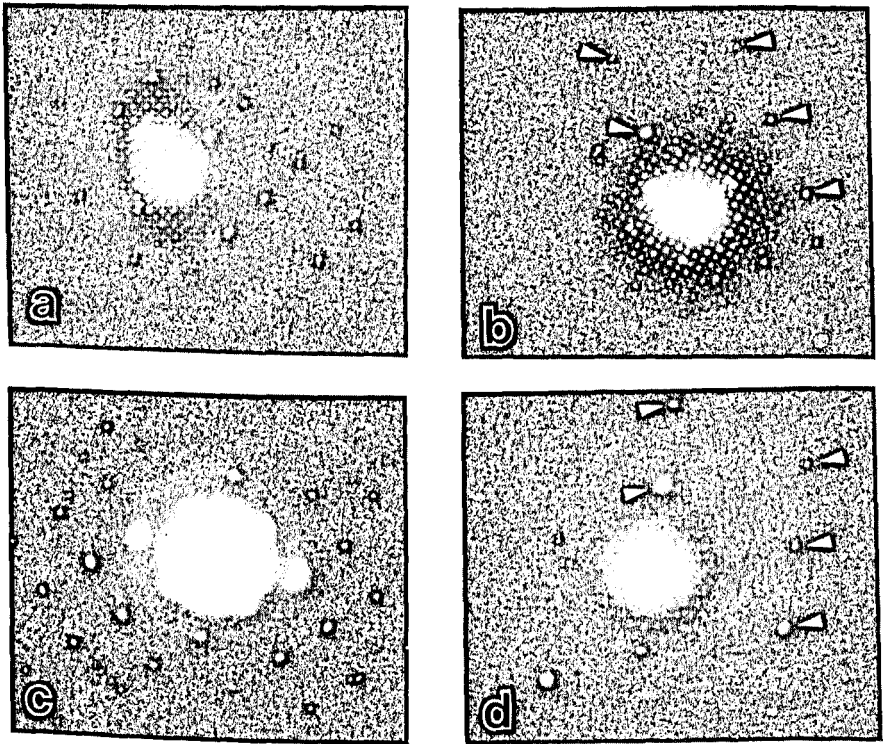


Figure 6: Electron diffraction patterns taken on several alpha-phase dispersoids. Each pattern allows to determine one type of orientation relationship. The arrows indicate the matrix spots when the matrix zone axis is not easy to identify.

- According to Fig. 6a:  $[111]Al // [001] \alpha$  and  $[01-1]Al // [010] \alpha$ ;  
 Fig. 6b:  $[31-1]Al // [-100] \alpha$  and  $[011]Al // [0-11] \alpha$ ;  
 Fig. 6c:  $[010]Al // [-1-13] \alpha$  and  $[103]Al // [1-10] \alpha$ ;  
 Fig. 6d:  $[31-1]Al // [111] \alpha$  and  $[103]Al // [0-11] \alpha$ .

and favors small and regular particles. Such properties are typically the ones which are desired to prevent from easy boundary migration. It is established that the pinning force on boundary is proportional to the density of particles and inversely proportional to their size [7].

### Concluding remarks

The two types of alpha-phase found in the 6013 alloy have been investigated. Regarding the interdendritic coarse alpha-phase particles, the main point is that they may contain, besides iron, quite a large amount of manganese. The manganese increase does not exactly induce a structure change but favors, by a long range ordering phenomenon, the transition from a Im3 to a Pm3 space group in a same crystal structure.

Concerning the alpha-phase forming dispersoids in the aluminum matrix, they show two main features. First, though Mn rich, they still contain some iron. The minimum ratio Mn/Fe is 3 regardless of the nominal composition of the alloys. Second, they exhibit several types of orientation relationships with the matrix. These crystallographic relations are likely to induce a beneficial effect on resistance to recrystallization.

### REFERENCES

1. R.A. Jenisky Jr., B. Thanaboonsombut and T.H. Sanders Jr, to be published in Metallurgical Transactions
2. M. Cooper, Acta Cryst. **23** (1967), 1106
3. M. Cooper and K. Robinson, Acta Cryst. **20** (1966), 614
4. H. Fowler, B. Mozer and J. Sims, Phys.Rev.B. **37** (1988), 3906
5. A.L. Mackay, Acta Cryst. **15** (1962), 916
6. P.Donnadieu, G.Lapasset and T.H. Sanders, Jr., submitted to Acta Cryst.
7. C.S. Smith, Trans.Metall.Soc., AIME, (1948)